Long-Term Variability in a Coupled Atmosphere–Biosphere Model

CHRISTINE DELIRE*

Center for Sustainability and the Global Environment (SAGE), Gaylord Nelson Institute for Environmental Studies, University of Wisconsin—Madison, Madison, Wisconsin, and Institut des Sciences de l'Evolution de Montpellier, Université Montpellier II, Montpellier, France

JONATHAN A. FOLEY

Center for Sustainability and the Global Environment (SAGE), Gaylord Nelson Institute for Environmental Studies, University of Wisconsin—Madison, Madison, Wisconsin

STARLEY THOMPSON

Lawrence Livermore National Laboratory, Livermore, California

(Manuscript received 15 December 2003, in final form 17 March 2004)

ABSTRACT

A fully coupled atmosphere–biosphere model, version 3 of the NCAR Community Climate Model (CCM3) and the Integrated Biosphere Simulator (IBIS), is used to illustrate how vegetation dynamics may be capable of producing long-term variability in the climate system, particularly through the hydrologic cycle and precipitation. Two simulations of the global climate are conducted with fixed climatological sea surface temperatures: one including vegetation as a dynamic boundary condition, and the other keeping vegetation cover fixed. A comparison of the precipitation power spectra over land from these two simulations shows that dynamic interactions between the atmosphere and vegetation enhance precipitation variability at time scales from a decade to a century, while damping variability at shorter time scales.

In these simulations, the two-way coupling between the atmosphere and the dynamic vegetation cover introduces persistent precipitation anomalies in several ecological transition zones: between forest and grasslands in the North American midwest, in southern Africa, and at the southern limit of the tropical forest in the Amazon basin, and between savanna and desert in the Sahel, Australia, and portions of the Arabian Peninsula. These regions contribute most to the long-term variability of the atmosphere–vegetation system.

Slow changes in the vegetation cover, resulting from a ''red noise'' integration of high-frequency atmospheric variability, are responsible for generating this long-term variability. Lead and lag correlation between precipitation and vegetation leaf area index (LAI) shows that LAI influences precipitation in the following years, and vice versa. A mechanism involving changes in LAI resulting in albedo, roughness, and evapotranspiration changes is proposed.

1. Introduction

Climate is known to vary at all time scales, and for many reasons (Mitchell 1976). Climatic variability can be due to external processes (e.g., diurnal and seasonal cycles, solar cycles, Milankovitch cycles), as well as internal mechanisms involving the interaction between the different components of the climate system. In theory, every geophysical process is capable of contributing to climate variability at one time scale or another (Mitchell 1976). Variations at time scales from seconds to seasons are mostly due to atmospheric processes, and the diurnal and seasonal cycle. Interannual and decadal variability were first thought to be the result of solar activity (Burroughs 1992) and are now also attributed to the interaction between atmospheric and oceanic processes, with the ocean acting as a long-term reservoir, damping fast variations in the atmosphere and favoring long-term ones (see, e.g., Ghil 2002).

It is interesting to note that the oceans are often considered the ''memory'' of the climate system, as they can enhance long-term variability in the climate system. Vegetation and soils, however, also operate on time scales of years to centuries and could therefore play an important role in climate variability on interannual, decadal, and

* Current affiliation: Institut des Sciences de l'Evolution, Université Montpellier II, Montpellier, France.

Corresponding author address: Christine Delire, Institut des Sciences de l'Evolution, CC 061, Université Montpellier II, Place E. Bataillon, 34095 Montpellier Cedex 5, France.
E-mail: delire@isem.univ-montp2.fr

© 2004 American Meteorological Society

Unauthenticated | Downloaded 12/05/21 03:12 AM UTC

centennial time scales. Perhaps the terrestrial biosphere can also act as a memory in the climate system?

Until recently, terrestrial ecosystems have received less attention than the oceans in the study of climate variability, especially at interannual to decadal time scales. Exceptions are the studies of the persistence of soil moisture anomalies (see Liu and Avissar 1999 for a review) and the possible effects of land cover changes on the persistence of the Sahel drought (Nicholson 2000).

But how might terrestrial systems act to enhance long-term climatic variability? One possibility is through soil moisture, which affects the atmosphere by altering the partitioning between the latent and sensible heating at the land surface (Delworth and Manabe 1988). As a result, the persistence of soil moisture affects the persistence and variability of atmospheric variables (Delworth and Manabe 1989), including precipitation. Delworth and Manabe (1988) showed with a bucket model coupled to a GCM that the anomalies of soil moisture persist for much longer than the anomalies of precipitation, implying that soil moisture acts as an integrator of rainfall at seasonal time scales. Liu and Avissar (1999) performed a more detailed study by using a GCM coupled to a biophysical land surface model explicitly taking into account the spatial distribution of different types of vegetation and soil. They found results similar to Delworth and Manabe—mainly that soil moisture and temperature have persistence on a seasonal time scale all over the globe with much stronger persistence in the case of soil moisture. Interestingly, neither study found indications of persistence of precipitation at time scales longer than a year. In both studies, however, the vegetation cover itself is taken as a fixed boundary condition. In reality, changes in vegetation cover happen at time scales of seasons (for leaf area) to years and decades (for changes in vegetation structure, and community composition). Taking these vegetation dynamics into account within climate models will most likely affect climate variability from seasonal to decadal time scales.

Recently, some studies of the Sahel region have demonstrated that vegetation feedbacks may play an important role in the decadal persistence of dry and wet periods. Over the last few centuries, the climate of the Sahel has been characterized by a succession of dry and wet periods, each lasting for several decades. In the rest of the world, however, wet and dry spells do not usually exceed 2–5 yr (Nicholson 2000). In a review of recent observational and modeling work, Nicholson (2000) shows how vegetation modulates land–atmosphere interactions by accelerating or delaying moisture transfer to the atmosphere. Wang and Eltahir (2000a–c) showed with a highly simplified atmospheric model coupled to a dynamic vegetation model simulating biophysical and biogeochemical processes that a change in the Atlantic sea surface temperatures off the coast of West Africa or an increase in land degradation in the Sahel alone are not sufficient to cause the persistent drought observed in the region since the 1970s, unless local feedbacks from changes in the vegetation cover are included. The slow response of the local vegetation cover must be included in the model in order to simulate a persistent drought. Using a different simple regional climate model coupled to a very simple dynamic vegetation model, Zeng et al. (1999) also showed that vegetation dynamics increases the interdecadal variability of precipitation over the Sahel triggered by changing sea surface temperatures in the tropical Atlantic.

Feedbacks between the vegetation and the atmosphere may also play an essential role on centennial time scales. Around 5500 yr before present, the climate of the Sahara abruptly switched from the wet conditions that prevailed during the early to mid-Holocene to the present desert conditions. Brovkin et al. (1998) and Claussen et al. (1999) showed with a climate system model of intermediate complexity how strong feedbacks between the vegetation dynamics and the climate are essential in simulating this abrupt climate change (Foley et al. 2003; Higgins et al. 2002; Scheffer et al. 2001).

In this study, we examine the effects of atmosphere–land surface–vegetation cover interactions on the variability of climate on time scales of longer than a year. We use a fully coupled atmosphere–vegetation model (including fully dynamic representations of land surface processes and changing vegetation cover) to analyze the effect of vegetation dynamics on the variability of the simulated climate.

Previous studies of the role of terrestrial systems in modulating global climatic variability have been performed either with 1) GCMs operating with fixed vegetation characteristics or 2) simplified atmospheric models, linked with dynamic vegetation models with different degrees of complexity. Very recently Wang et al. (2004) used a dynamic vegetation model coupled to a GCM to study the Sahel region. To our knowledge, this is the only study of its kind. However, it is mostly focused on the Sahel region, while our analysis is global. By using an atmospheric GCM coupled to a fully dynamic global vegetation model we can analyze the global-scale effects of vegetation dynamics on the variability of the climate system.

2. The coupled atmosphere–vegetation model

In this study, we use the National Center for Atmospheric Research (NCAR) Community Climate Model version 3 (CCM3; Kiehl et al. 1998) coupled with an updated version of the Integrated Biosphere Simulator (IBIS) of Foley et al. (1996) and Kucharik et al. (2000). We refer to this coupled model as CCM3–IBIS (Delire et al. 2002, 2003).

CCM3 is a general circulation model of the atmosphere with spectral representation of the horizontal fields. The model has 18 levels in the vertical and operates with a 20-min time step. In its original form,

Unauthenticated | Downloaded 12/05/21 03:12 AM UTC

CCM3 is coupled to the Land Surface Model (LSM) of Bonan (1998). We have replaced the LSM land surface package with the IBIS land surface/terrestrial ecosystem model (Delire et al. 2002). The model operates at a resolution of T31 (the spectral representation of the horizontal fields is truncated at the 31st wavenumber using a triangular truncation; horizontal fields are converted to a $\sim 3.75^\circ \times 3.75^\circ$ grid).

The global terrestrial biosphere model IBIS (version 2) is a comprehensive model of terrestrial biospheric processes, and simulates land surface physics, canopy physiology, plant phenology (budburst and senescence), vegetation dynamics (accumulation and turnover of carbon, and competition between plant functional types), and carbon cycling. Land surface physics and canopy physiology are calculated with the time step used by the atmospheric model (20 min). The plant phenology algorithm has a daily time step and the vegetation dynamics is solved with an annual time step. In these simulations, IBIS operates on the same T31 spatial grid as the CCM3 atmospheric model.

The land surface module in IBIS simulates the full energy, water, carbon, and momentum balance of the soil–vegetation–atmosphere system. The module is based on the land surface transfer scheme (LSX; Thompson and Pollard 1995a,b). The module describes two vegetation layers (i.e., ''trees'' and ''grasses and shrubs'') and six soil layers to simulate soil temperature, soil water, and soil ice content over a total depth of 4 m. Physiologically based formulations of C3 and C4 photosynthesis (Collatz et al. 1991; Farquhar et al. 1980), stomatal conductance (Collatz et al. 1992), and respiration (Amthor 1984) are used to simulate canopy gas exchange processes. This approach provides a mechanistic link between the exchange of energy, water, and CO_2 between vegetation canopies and the atmosphere. Budburst and senescence depend on climatic factors following the empirical algorithm presented by Botta et al. (2000).

The vegetation dynamics module calculates the evolution of 12 plant functional types (PFTs) competing for light and water using the calculated annual carbon balance. IBIS represents vegetation dynamics using very simple competition rules. The relative abundance of the 12 PFTs in each grid cell changes in time according to their ability to photosynthesize and use water. For example, in a grid cell where trees and grasses coexist, grasses are shaded by trees but their rooting profile allows them to withdraw water first as it infiltrates through the soil. In drought conditions, grasses will be favored, while trees will accumulate less carbon, will grow fewer leaves, and will eventually wilt. In wet conditions, trees will grow faster and shade the grasses. Competition among grass types or among tree types results from different allocation strategies, phenology, type of leaf, or type of photosynthesis leading to different annual carbon balances.

IBIS has been tested against site-specific biophysical measurements from flux towers (Delire and Foley 1999), field-level ecological studies (Kucharik and Brye 2003; Kucharik et al. 2001), as well as spatially extensive ecological (Kucharik et al. 2000) and hydrological data (Costa and Foley 1997; Lenters et al. 2000).

IBIS is explicitly designed to work within atmospheric models. The model has been first coupled to the Global Environmental and Ecological Simulation of Interactive Systems (GENESIS) climate model and used to study climate vegetation interactions (e.g., Foley et al. 1998, 2000; Levis et al. 1999a–c, 2000). We have recently coupled IBIS to the NCAR CCM3 climate model (Kiehl et al. 1998) by replacing the original land surface scheme LSM of Bonan (1998). The climate simulated by CCM3–IBIS is analyzed and compared against observations and the results of the standard CCM3–LSM model in Delire et al. (2002).

3. Simulation design

To examine the role of vegetation dynamics in the long-term variability of the climate system, we conducted two long simulations with CCM3–IBIS. In the first simulation, the dynamics of the vegetation cover was predicted, so that the vegetation itself interacted with the climate. In the second simulation, the vegetation cover was assumed to be fixed, and was prescribed for each grid cell according to the average results of the first model simulation. Therefore, feedbacks between the vegetation distribution and the atmosphere are not taken into account in the second simulation. Differences in climate variability between the two simulations are due only to the interaction between the dynamic vegetation cover and the atmosphere. Herein, we will refer to the first simulation as the dynamic vegetation simulation and to the second simulation as the fixed vegetation simulation.

We ran the dynamic vegetation simulation for 480 yr, at a resolution of T31 for present-day conditions (modern orbital conditions, 1367 W m^{-2} solar constant, and 350 ppmv CO_2). To limit computing costs, we accelerated the vegetation dynamics module for the first 20 yr so that it achieved 150 yr during the 20 yr of actual atmospheric model simulation. The vegetation dynamics module, which normally operates at a yearly time step, was called 10 times during the first 10 yr of simulation. A linear decrease in the degree of acceleration was applied during the next 10 yr until model year 21, when the vegetation dynamics module was called once a year. This was needed because vegetation dynamics are slow processes: it takes decades to centuries for a boreal forest to grow and reach equilibrium. Because the soil carbon has a very long characteristic time scale, we also accelerated the soil carbon module for the first 100 yr so that the soil carbon achieves 3500 yr during the 100 first years of the run [see Kucharik et al. (2000) for a detailed description of the acceleration procedure]. To limit the effect of initial conditions and acceleration on

Unauthenticated | Downloaded 12/05/21 03:12 AM UTC

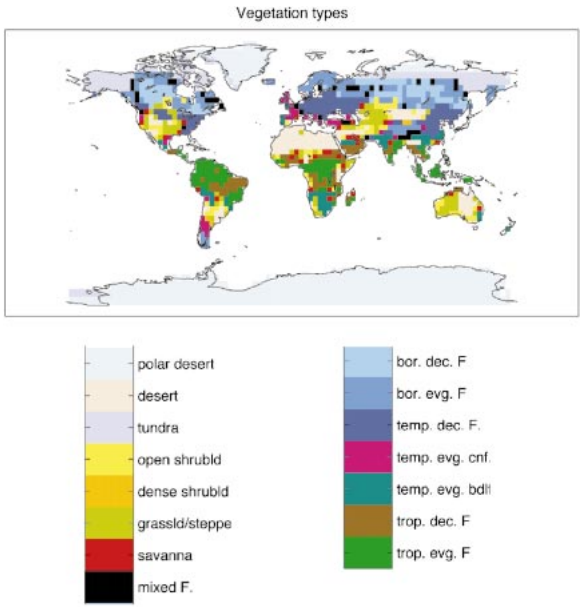

FIG. 1. Distribution of vegetation types simulated by CCM3–IBIS. The most frequent vegetation types for the last 50 yr of the dynamic vegetation run are presented.

our results, we only used the last 260 yr of the 480-yr run for our analysis. The average climate, vegetation distribution, and carbon cycle from these years are described in Delire et al. (2003).

In the fixed vegetation simulation, run for 160 yr, the vegetation cover was prescribed in each grid cell and stayed constant during the entire run. The prescribed vegetation type was the most frequent vegetation type simulated in the last 50 yr of the dynamic vegetation simulation (Fig. 1). As described in Delire et al. (2003), IBIS calculates once a year a diagnostic map of the vegetation-type distribution based on the relative abundance of PFTs in each grid cell and some climatic rules. We determined the most frequent vegetation type occurring during the last 50 yr of the first simulation and initialized the fixed vegetation simulation with this vegetation cover. We chose to use the last 50 yr of the dynamical vegetation run because they correspond to the results described in Delire et al. (2003). Using the whole time series (260 yr) might result in a slightly different mean state of the climate and vegetation but should not affect climate variability. Similarly, the vegetation cover imposed in the fixed vegetation simulation is not exactly the one experienced by the model in the dynamic vegetation simulation because of averaging issues, but this should not affect climate variability. Prescribing the vegetation in IBIS means that the relative abundance of the 12 plant functional types is fixed in each grid cell. All the carbon pools are identical from one year to another, while the annual mean vegetation cover and the peak leaf area index (LAI) reached during the year are constant. Budburst, leaf growth, and senescence, however, still depend on the climate during the course of the year. The amplitude of the seasonal cycle of LAI is thus identical each year, but its shape varies from year to year according to the climate. This change in the seasonal cycle of leaf display affects the atmosphere. Feedbacks between the vegetation and the atmosphere are thus not completely neglected: they are taken into account during the seasonal cycle of leaf phenology, but neglected from year-to-year variations in canopy cover or vegetation structure. With the vegetation cover prescribed, the coupled model reached equilibrium in a few years. We used the last 150 yr of this run for our analysis.

In both simulations, fixed climatological sea surface temperatures (SSTs) were used. The soil texture dataset used in the coupled model CCM3–IBIS was the International Geosphere-Biosphere Programme–Data and Information System (IGBP–DIS; Global Soil Data Task Group 2000) global gridded texture database interpolated to T31 resolution. The model vegetation was initialized with modern natural vegetation (Ramankutty and Foley 1999).

4. Variability in precipitation

We first analyze the behavior of long-term climatic variability in our coupled simulations, primarily focusing on precipitation variability. Previous analyses have demonstrated how changes in vegetation cover can induce large changes in the hydrologic cycle and precipitation patterns (see Bonan 2002 for a review).

a. Spectral analysis

We first compare the time series of annual precipitation of both simulations in the frequency domain. Precipitation over land has a very different spectral signature in the dynamic vegetation case than in the fixed vegetation case (Fig. 2). Overall, the power spectrum of precipitation (calculated as the area average of the local power spectra) in the fixed vegetation case is flat, with slightly decreasing power at low frequencies. It resembles that of a white noise process, indicating a system with variability at all time scales and little or no memory (Hasselmann 1976).

The power spectrum of precipitation over land in the dynamic vegetation simulation, however, is mainly flat at frequencies from 0.5 to 0.1 cycles per year (cpy; corresponding to time scales of 2–10 yr) and increases at frequencies between 0.1 and 0.009 cpy (10 and 110 yr), while decreasing at lower frequencies. Except for frequencies lower than 0.009 cpy, the overall shape of the dynamic vegetation precipitation spectrum is characteristic of a ''red noise'' process, indicating a system with variability at all time scales but with a long-term memory (Hasselmann 1976). In this case the time scale of the long-term memory is between 10 and 110 yr. Because the sea surface temperatures are fixed in our simulation, the only processes with a long-term memory

Unauthenticated | Downloaded 12/05/21 03:12 AM UTC

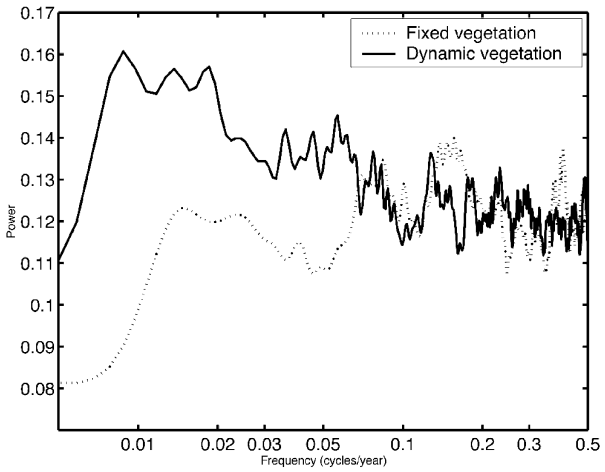

FIG. 2. Power spectra of simulated precipitation areally averaged over land. The solid line is from the dynamic vegetation simulation and the dotted line is from the fixed vegetation simulation. The power spectra are calculated using the multitaper method (Ghil et al. 2002).

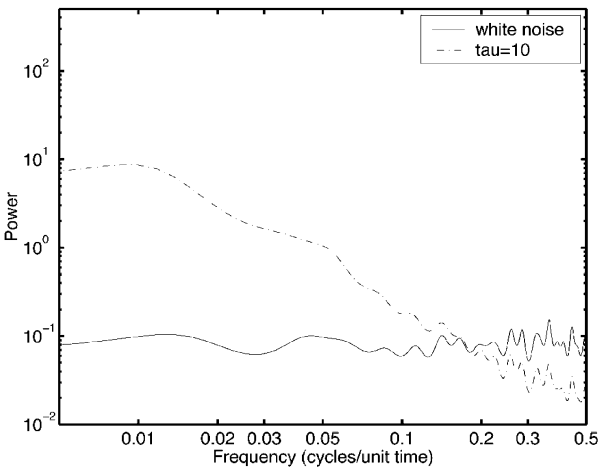

FIG. 3. Power spectrum of a white noise generated by a random number generator and a damped oscillator with a characteristic time scale (tau) of 10-unit time. The power spectrum is calculated using the maximum entropy method (the multitaper method gives the same overall result).

are the vegetation dynamics and, to a lesser extent, soil moisture and the accumulation of snow in Antarctica and Greenland. However, snow and soil moisture are also calculated in the fixed vegetation simulation and cannot explain the difference between the two spectra. Vegetation dynamics is thus responsible for the red noise shape of the spectrum. This means that the dynamics of vegetation induces low-frequency variability in the precipitation at time scales from 10 to 110 yr.

At frequencies between 0.08 and 0.5 cpy (~12 and 2 yr), the power from the fixed vegetation simulation is often higher than the power from the dynamic vegetation simulation. This is because the dynamic vegetation damps the variations at higher frequencies (up to 0.5 cpy). This behavior is similar to the power spectrum of a damped stochastic oscillator where the stochastic oscillation is given by a white noise. To illustrate the similarity between the behavior of the atmosphere–vegetation system in CCM3–IBIS and the oscillator, Fig. 3 presents the power spectrum of a white noise (approximated by a random number generator) and a damped stochastic oscillator as obtained from

$$\frac{dy(t)}{dt} = wn - \frac{y(t)}{\tau},$$

where wn is the white noise, τ is the characteristic time scale (the memory), and y the damped oscillator. The spectrum of the white noise is mainly flat while the spectrum of the damped oscillator increases at low frequencies and decreases at high frequencies (Fig. 3).

In our model atmosphere–vegetation system, the fast atmospheric components play the role of the random forcing in the stochastic oscillator while the slowly responding vegetation dynamics is the integrator and damping mechanism. This dampening of high-frequency variability was also found by Wang and Eltahir (2000c) when studying the role of vegetation dynamics in the variability of the Sahel rainfall.

We performed this analysis with annual mean precipitation because we were interested in the influence of vegetation dynamics on the long-term variability of the climate system. Vegetation–atmosphere interactions also occur at much faster time scales however and could therefore also affect the variability of the precipitation at weekly to monthly time scales.

b. Variability and persistence

The spectra presented in the previous section give a global view of precipitation variability. Another measure of the temporal variability of precipitation is the lagged autocorrelation coefficient, which indicates whether anomalies of precipitation persist. If the atmosphere were isolated from the earth's surface, an atmospheric anomaly should only persist for about 2 weeks because there are no tropospheric processes with time scales longer than 2 weeks (see, e.g., Barry and Carleton 2001). Persistence of atmospheric anomalies over longer periods, first described by Namias (1952), is therefore due to external forcing or the interaction between the land and ocean and the atmosphere. In our two simulations only the land surface can induce atmospheric persistence.

At each grid point, and for both simulations, we compute the correlation coefficient of the time series of annual precipitation with itself, but lagged 1 and 5 yr. As expected, very few regions present significant 1- and 5-yr-lagged autocorrelations of their time series of precipitation with the fixed vegetation simulation (Figs. 4a,b). Indeed, except for high-latitude snow and soil processes, there are no processes with annual time scales in the land–atmosphere system when the vegetation cov-

Unauthenticated | Downloaded 12/05/21 03:12 AM UTC

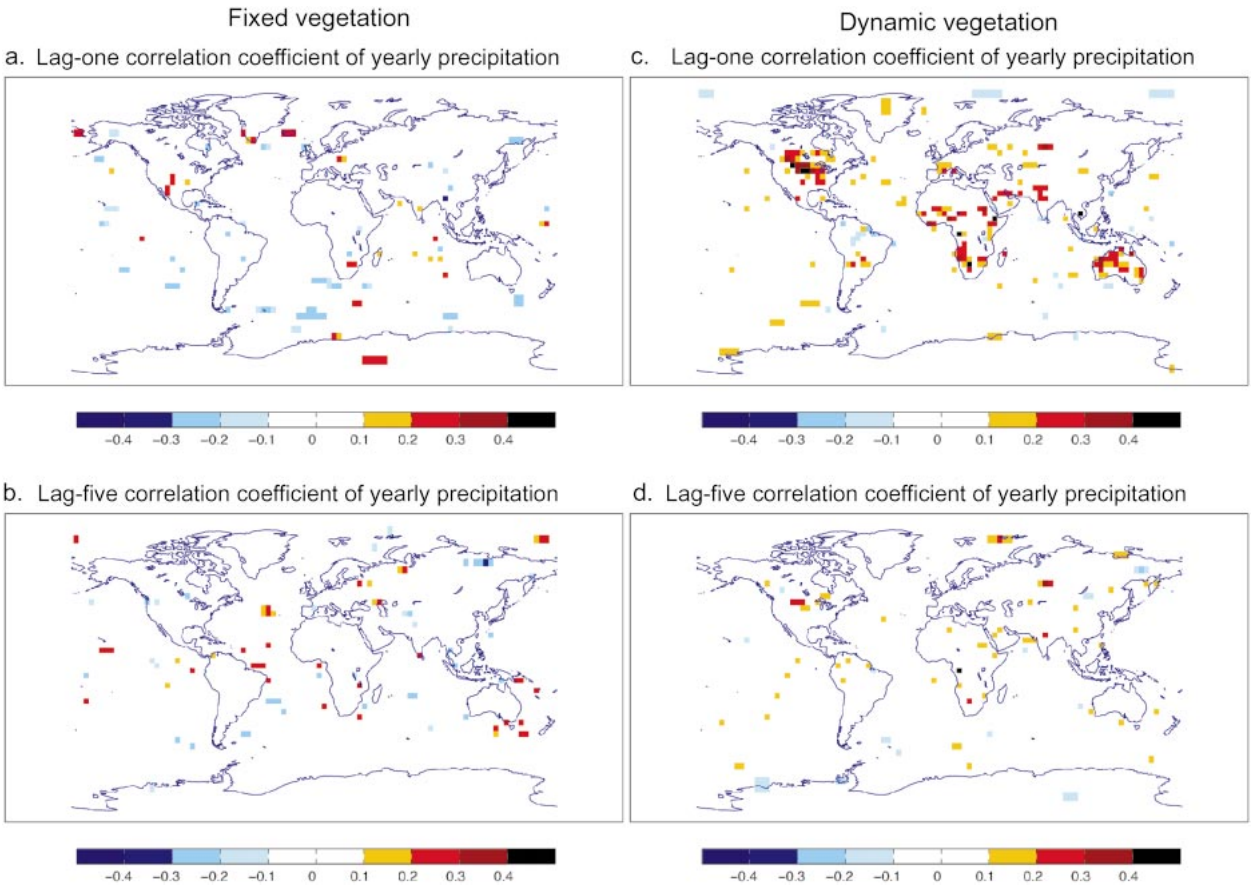

FIG. 4. Lagged autocorrelation coefficient of the yearly precipitation time series for (a) the fixed vegetation simulation with a 1-yr time lag and (b) with a 5-yr time lag, and for (c) the dynamic vegetation simulation with a 1-yr time lag and (d) with a 5-yr time lag. The values displayed are significant at the 99% confidence level using a Student's *t* test.

er is fixed. This result agrees with Delworth and Manabe (1989) and Liu and Avissar (1999) who only found persistence of the precipitation anomalies at monthly time scales with a GCM coupled to a land surface model where the vegetation cover is fixed.

In the dynamic vegetation simulation, the 1-yr-lagged autocorrelations are mostly positive over land, showing that anomalies of precipitation persist on yearly time scales (Fig. 4c). The regions with positive autocorrelation coefficients are the Great Lakes region in United States and Canada; the southern limit of the Amazon basin; portions of western Europe; the Sahel, South Africa, and Namibia; portions of the Arabian Peninsula; northern India; Australia; and a few regions in central Asia.

Most of these regions correspond to transitions between very different ecosystems in the model—mainly transitions between forests and grasslands or between grasslands and deserts (Fig. 1). The region with positive autocorrelation in the midwestern United States and Canada is at the limit between deciduous forest and grassland and shrubland to the south and east, and at the limit between deciduous forest and boreal forest to the north. In South America, the region is a transition between tropical deciduous forest, temperate evergreen forest, grassland, and shrubland. In southeast Africa, the region with positive autocorrelation is at the limit between temperate evergreen forest and grassland and shrubland. In the Sahel and the Arabian Peninsula, the vegetation cover ranges from tropical forest, to savannas and grasslands, ultimately to desert. In Australia, the region has grassland, semidesert, and desert. In Eurasia, anomalies of precipitation persist mainly at the limit between forest types: boreal deciduous and boreal evergreen or temperate deciduous and temperate evergreen.

With the exception of Eurasia, the limit between these ecosystems depends on water availability; grasslands require less moisture than forests, but more than deserts. It is logical that the limit between a water-limited and a non-water-limited ecosystem will be the most sensitive to variations in rainfall.

The equatorial regions show very little persistence. This result, in agreement with Delworth and Manabe (1989) and Liu and Avissar (1999), confirms that the observed long-term variability and persistence of the

Unauthenticated | Downloaded 12/05/21 03:12 AM UTC

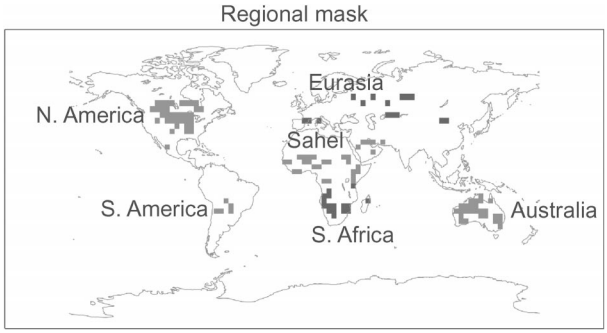

FIG. 5. Regional masks obtained from Fig. 4c. The masks contain the grid cells where the absolute value of the lag-1 autocorrelation coefficient of the precipitation is higher than 0.1 and significant at the 99% level.

precipitation in these regions (Hastenrath 1991) are most likely due to the interaction between the ocean and the atmosphere.

The 5-yr-lagged autocorrelation is also positive over land indicating that anomalies persist at least for 5 yr in certain areas, but the area with significant autocorrelation is smaller than for the 1-yr lag (Fig. 4d).

We used the map of 1-yr-lagged autocorrelation to define regional geographical masks (Fig. 5) to calculate area averages of the power spectra over them (Fig. 6). As expected, the precipitation in all these regions presents strong red noise characteristics in the dynamic vegetation simulation. Superimposed on the red noise are some peaks at decadal time scale indicative of an oscillatory behavior of the precipitation within the region. Decadal variability of the precipitation has been documented in the literature for the Midwest in North America (Burroughs 1992; Hu et al. 1998) and the Sahel (see, e.g., Nicholson 2000).

5. Variability in vegetation cover and land surface characteristics

Next we examine the long-term variability of the vegetation cover and the associated change in land surface characteristics, which are linked to changes in precipitation.

a. Vegetation cover

In IBIS, the peak leaf area index (LAI) reached during the year is a reasonable indicator of the vegetation's behavior on year-to-year time scales. LAI depends on the amount of carbon assimilated by each plant functional type (PFT) and is therefore dependent on the climatic conditions. We use peak LAI instead of biomass to describe the state of the biosphere because it is the vegetation characteristic that most influences the atmosphere–biosphere interactions of energy and water exchange. LAI strongly affects the albedo of the surface, as well as the evapotranspiration rate and the roughness of the surface, which can all affect the climate. It also has the fastest time scale of the vegetation cover, compared to long-lived biomass and soil carbon pools. After a disturbance, leaf production is very high so that a 10-yr-old secondary forest can have the same LAI as a 400-yr-old mature forest (Bonan 2002). In contrast, biomass accumulation is much slower.

The persistence of peak LAI anomalies measured by the lagged autocorrelation coefficient (not shown) is much higher than the persistence of precipitation and the power spectrum has the characteristics of a red noise with very long memory (not shown). We use Manabe and Stouffer's approach (Manabe and Stouffer 1996) to analyze in another simple way the variations in time of the peak LAI: we average the time series of LAI over nonoverlapping consecutive intervals of 1, 5, and 25 yr, thereby removing most of the variation at time scales shorter than 2, 10, and 50 yr. The variability at different time scales is illustrated by the standard deviation of the annual, and 5- and 25-yr mean values. The peak LAI shows similar patterns of variability at all three time scales with smaller amplitude at longer time scales (Fig. 7). The higher values are found in the northern part of the Great Lakes region of the United States and Canada, at the southern border of the Amazon basin, in the Sahel and the Arabian Peninsula, in South Africa, in India and Southeast Asia, and around 60°N in Eurasia. This means that vegetation, characterized by the peak LAI, varies at time scales up to 50 yr, especially in these particular regions. With the exception of Eurasia, these regions correspond to the zones where the anomalies of precipitation persist for more than a year (the spatial correlation between Fig. 7 and Fig. 4c is 0.44 over all land cells, 0.49 from 68°N to 68°S, and 0.5 from 53°N to 53°S). In Eurasia, the variability of the LAI is more linked to changes in temperature and cloudiness as the mid- to northern latitude vegetation types are more directly controlled by changes in temperature and radiation (Nemani et al. 2003).

In the Sahel, the standard deviation of peak LAI ranges between 0.2 and 1 (coefficient of variation between 30% and 90%). The standard deviation of yearly precipitation in the same region (not shown) varies between 0.2 and 0.4 mm day^{-1} (coefficient of variation between 25% and 90%). Those values are similar to those obtained by Wang and Eltahir (2000a) when studying the impact of a perturbation in vegetation in the Sahel region.

As in the case of the persistence of precipitation anomalies, the regions with higher peak LAI variability correspond to transitions between different ecosystems in the model. Long-term variability in vegetation is most likely to occur in transition zones between ecosystems. A slight variation of the general circulation will be sufficient to move this boundary and strongly impact the local vegetation cover. In the Sahel, for instance, where the climate varies from tropical humid to desertic in a few hundred kilometers along a south–north transect, a

Unauthenticated | Downloaded 12/05/21 03:12 AM UTC

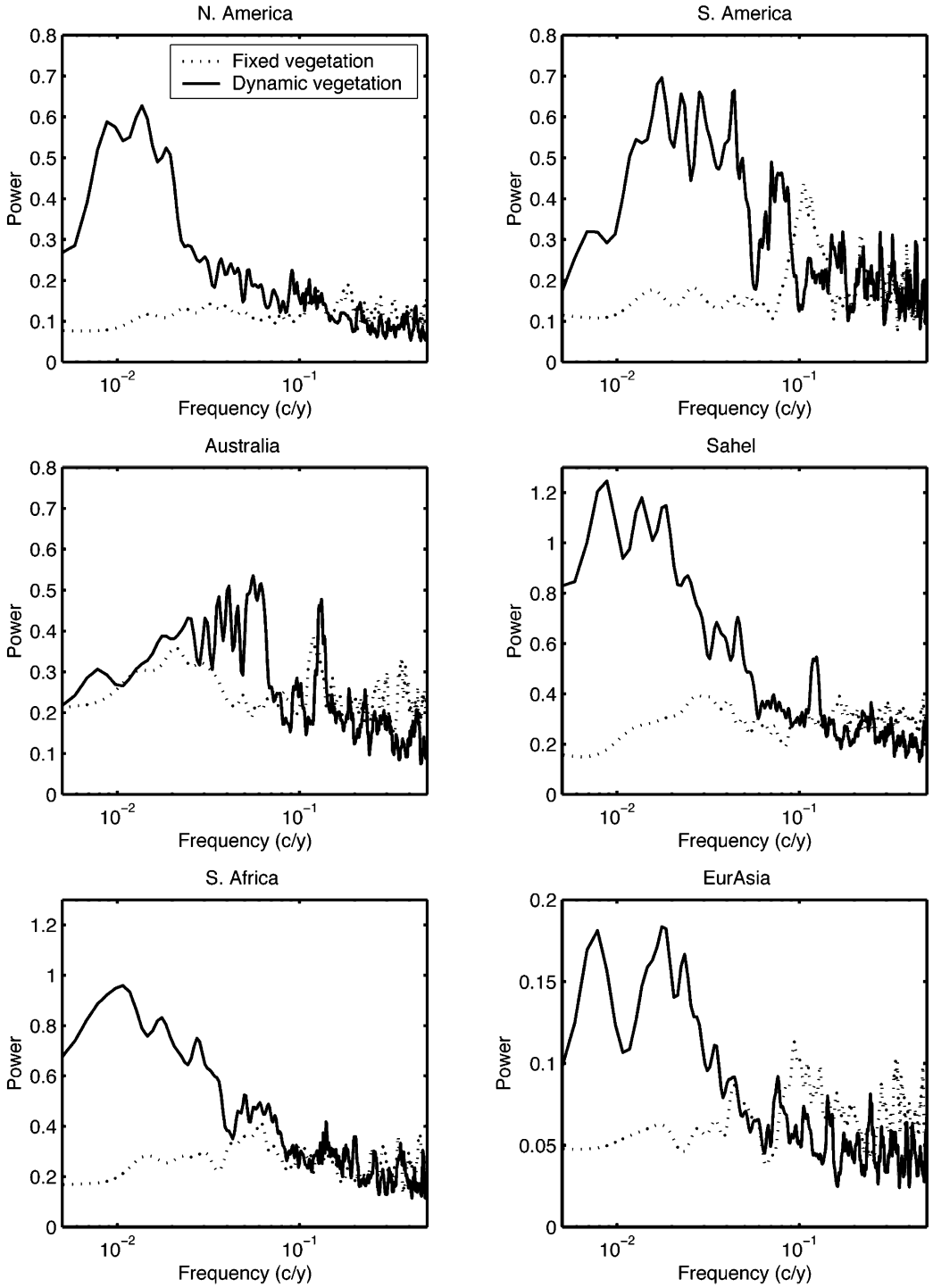

FIG. 6. Power spectra of simulated precipitation areally averaged over the masks defined in Fig. 5. The solid line is from the dynamic vegetation simulation and the dotted line is from the fixed vegetation simulation.

slight shift (~hundred kilometers) in the extent of the monsoon rainfall has a strong impact on the local vegetation. This is as opposed to the center of an ecosystem, where a long-term change in vegetation would require a major change in the climate.

Furthermore, a change in vegetation between two very different ecosystems (e.g., forest versus grassland) will have more physical impact on the atmosphere than a change in vegetation between similar ecosystems (e.g., two different forest types). The changes in albedo, in

Unauthenticated | Downloaded 12/05/21 03:12 AM UTC

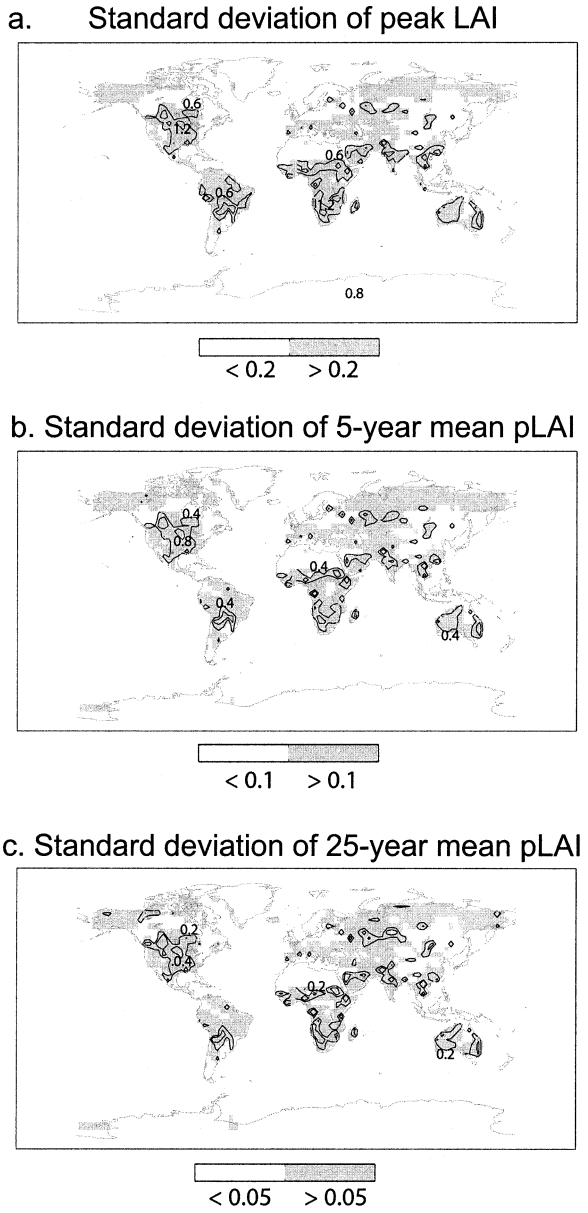

FIG. 7. Standard deviation of the peak leaf area index. (a) Standard deviation of yearly pLAI, (b) standard deviation of 5-yr mean pLAI, and (c) standard deviation of 25-yr mean pLAI. The 5- and 25-yr means of pLAI are averages of the pLAI time series over nonoverlapping consecutive intervals of 5 and 25 yr. Regions in light gray have standard deviation higher than 0.2 (respectively, 0.1 and 0.05 for the 5- and 25-yr mean). The superimposed contours indicate regions where the deviation is larger: 0.6 and 1.2 for the 1-yr mean, 0.4 and 0.8 for the 5-yr mean, and 0.2 and 0.4 for the 25-yr mean.

roughness, and leaf area index are much bigger in the case of a grassland replaced by a forest, for example, than in the case of a tropical evergreen forest replaced by a tropical deciduous forest. The larger the changes in the surface physical characteristics, the larger the impact on the climate and, in this case, on the precipitation. Ecotones are thus likely to exhibit long-term variability because they are at the boundary between very different climates and this boundary can easily shift. A change in this boundary will trigger changes in vegetation types that have very different physical characteristics and are thereby more likely to affect the atmospheric circulation. An analog of these transition zones in an atmosphere–ocean system would be the zones where SSTs are affected by long-term oceanic internal processes like the tropical Pacific with ENSO, the North Atlantic, or the circumpolar Arctic.

To determine whether slow changes in vegetation cover are linked to the long-term variability in the precipitation, we calculate lag and lead correlations between peak LAI and precipitation (Fig. 8). The maximum correlation is obtained for a zero lag between the annual LAI and precipitation. The correlation remains high when the peak LAI lags the precipitation by 1 yr, and decreases with a lag of 5 yr. Correlation coefficients between peak LAI and precipitation when LAI leads the precipitation are low, but not negligible, indicating that peak LAI indeed has an influence on the local precipitation in the model at time scales of 1–5 yr. They are smaller than when LAI lags the precipitation but they are significant in large regions of the world. It is not surprising that the correlation with peak LAI leading precipitation is smaller than in the case where LAI lags precipitation because precipitation affects vegetation locally while vegetation can affect the precipitation both locally and over a larger region through changes in the atmospheric circulation.

The regions where the correlation between the peak LAI of 1 yr and the precipitation of the subsequent year are high are the same as the regions where precipitation anomalies show strong persistence. One could argue that the correlation between one year's LAI and the following year's precipitation could be simply due to the persistence of the precipitation and the high correlation (at lag 0) between precipitation and peak LAI. We know, however, from the fixed vegetation simulation that there is almost no persistence in the precipitation field when feedbacks from the vegetation dynamics are not taken into account. Therefore, the significant correlation between the LAI of 1 yr and the precipitation of the next indicates a causal effect between changes in LAI and changes in precipitation.

b. Land surface characteristics

Because the atmosphere and the biosphere are coupled in our simulations, it is very difficult to identify detailed mechanisms responsible for the long-term variability of the precipitation. We can, however, illustrate potential atmosphere–vegetation feedback mechanisms linked to changes in albedo and evapotranspiration.

As mentioned earlier, the LAI influences the albedo of the surface, its roughness, and the evapotranspiration rate. Except in the high latitudes, the patterns of variation of the standard deviation of the albedo (Figs. 9a–

Unauthenticated | Downloaded 12/05/21 03:12 AM UTC

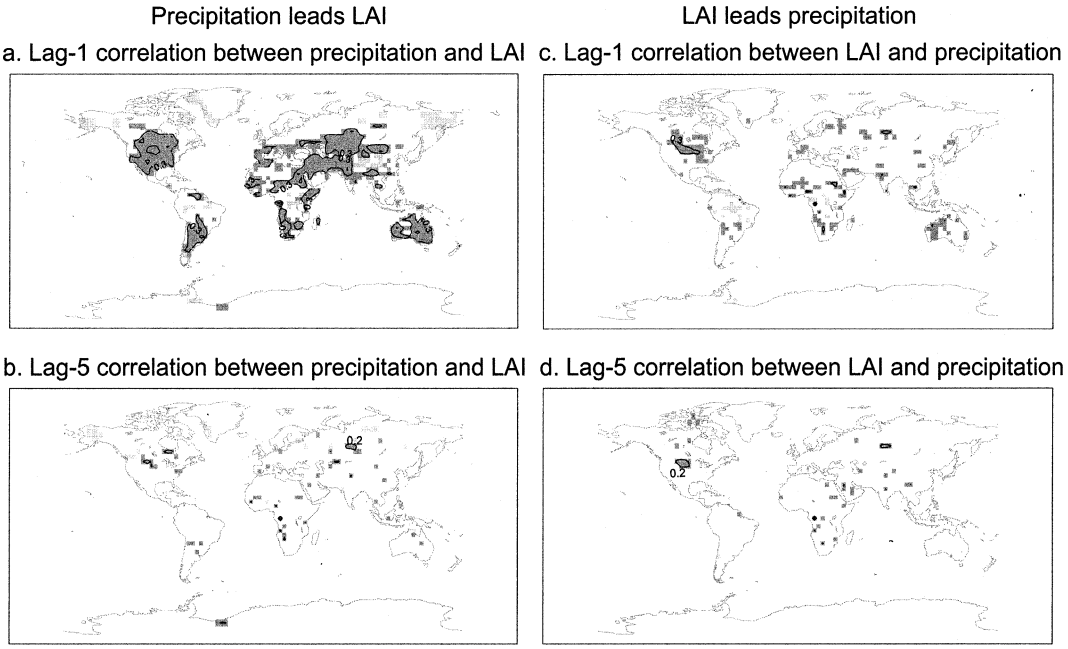

FIG. 8. Correlation between precipitation and peak LAI. (a) Precipitation leads pLAI by 1 yr (contour interval of 0.3), (b) precipitation leads pLAI by 5 yr (contour interval of 0.2), (c) precipitation lags pLAI by 1 yr (contour interval of 0.3), and (d) precipitation lags pLAI by 5 yr (contour interval of 0.2). The shading indicates values significant at the 99% level. Regions in light (dark) gray have negative (positive) correlation.

c) are very similar to the pattern of variation of the standard deviation of the peak LAI, with higher values in the Midwest, south of the Amazon basin, in the Sahel and Saudi Arabia, in southwest Africa, in central Asia, and in Australia. This remains true at the 10- and 50-yr time scales. The variability of the albedo is the largest in the high latitudes and mountainous regions because of the high albedo of the snow.

The evapotranspiration rate depends on the availability of soil moisture (and therefore precipitation), radiation, and LAI. Interestingly, the standard deviation of the evapotranspiration (Figs. 9d–f) varies in ways similar to the standard deviation of the peak LAI, but different from the standard deviation of precipitation, especially in the wet Tropics (Figs. 9g–i). This indicates that LAI controls the variability of the evapotranspiration. In the wet Tropics, precipitation is not a limiting factor to plant growth, so that LAI and evapotranspiration are fairly independent of precipitation. In areas where precipitation is limiting, LAI and therefore the evapotranspiration rate vary in response to the precipitation. This corroborates the hypothesis that precipitation anomalies trigger some long-term responses in the vegetation that feed back to the climate through biophysical processes such as changing albedo and evapotranspiration.

6. Summary and conclusions

In this paper, we examined the effects of vegetation dynamics on long-term climate variability. We performed two simulations of the present-day climate with a coupled climate–biosphere model, using fixed climatological sea surface temperatures: one of the simulations taking into account vegetation cover dynamics and the other keeping vegetation cover fixed.

Our spectral analysis of simulated precipitation over land shows that vegetation dynamics enhance the low-frequency variability of the biosphere–atmosphere system at time scales from a decade to a century, while damping higher-frequency variability. With fixed vegetation cover, the power spectrum of annual precipitation is mainly flat indicating similar variability at all time scales.

We also show that anomalies of precipitation persist for more than a year in large areas of the world when vegetation cover interacts with the atmosphere. Without the memory of the dynamic vegetation cover, anomalies of precipitation only persist for a few months. These persistent precipitation anomalies tend to occur in transition zones between very different ecosystems: between forest and grasslands in the Great Lakes region of the United States and Canada, at the southern limit of the Amazon basin and in South Africa, or between savanna and desert in the Sahel, Australia, and portions of the Arabian Peninsula.

Vegetation cover (measured through changes in peak LAI) also presents higher variability at time scales of up to 50 yr in roughly the same transitional regions. Lead and lag correlations between local peak LAI and local precipitation confirm that precipitation strongly

Unauthenticated | Downloaded 12/05/21 03:12 AM UTC

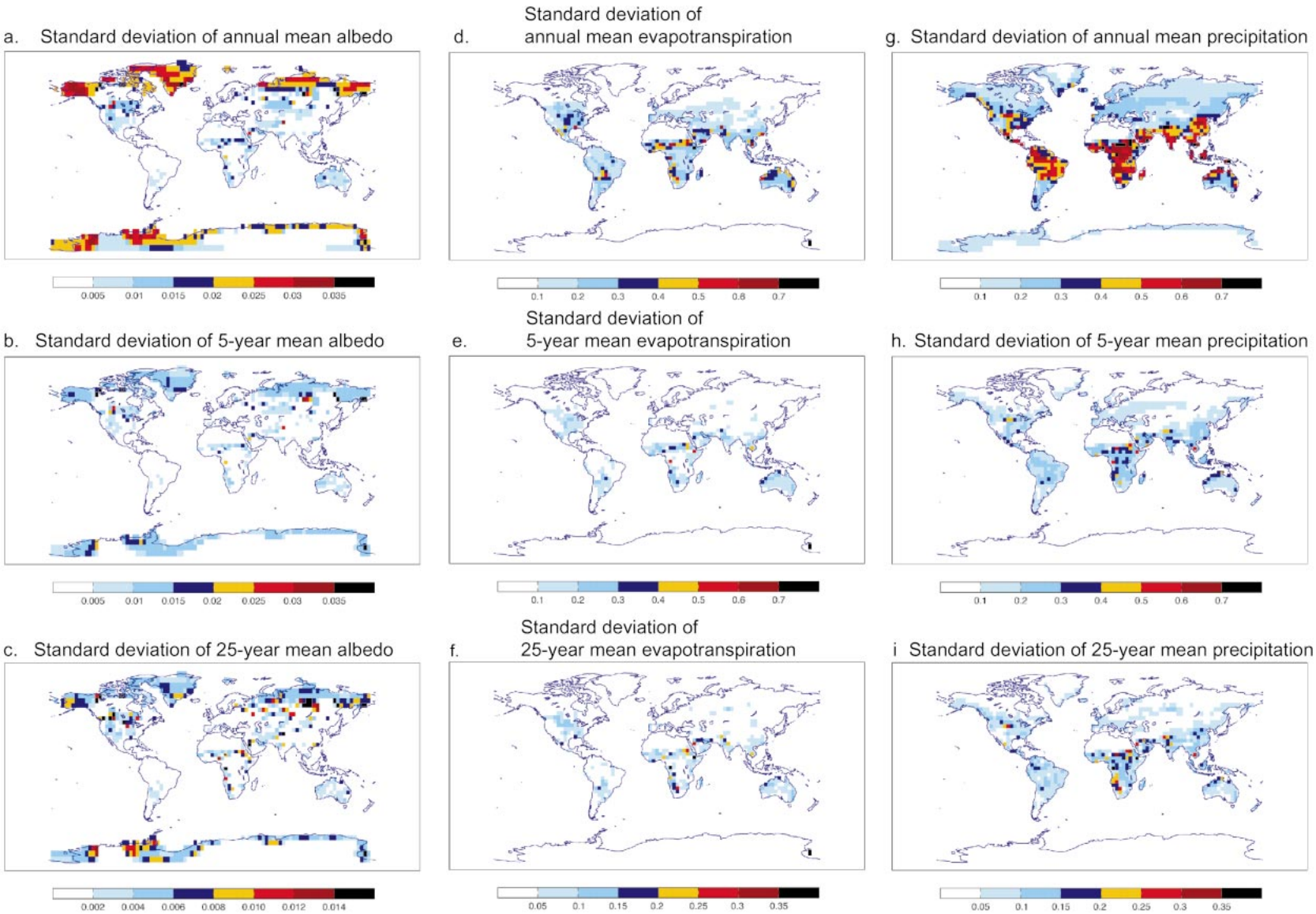

FIG. 9. Standard deviation of (a) annual mean albedo, (b) 5-yr mean albedo, (c) 25-yr mean albedo, (d) annual mean evapotranspiration, (e) 5-yr mean evapotranspiration, (f) 25-yr mean evapotranspiration, (g) yearly precipitation, (h) 5-yr mean precipitation, and (i) 25-yr mean precipitation. The 5- and 25-yr means are averages of the time series over nonoverlapping consecutive intervals of 5 and 25 yr.

Unauthenticated | Downloaded 12/05/21 03:12 AM UTC

affects the peak LAI of the current and following years, with decreasing influence in time. These lag correlations also show, however, that peak LAI affects future precipitation. LAI directly affects the albedo, the evapotranspiration rate, and the roughness of the land surface—variables that are known to affect the precipitation in many parts of the world. Except in high latitudes and mountainous areas, the geographical patterns of albedo variability are similar to that of peak LAI. The spatial distribution of the evapotranspiration variability is also similar to that of LAI, but it differs from the pattern of precipitation variability, indicating that vegetation cover and not precipitation controls the variability of evapotranspiration at longer time scales.

Because we ran the model with fixed climatological sea surface temperatures, we cannot expect the model to reproduce the observed interannual to decadal variability of the precipitation, especially in the Tropics. However, the variability simulated by the model at these scales in certain regions suggests that the biosphere–atmosphere system may be a primary driver of long-term variability in these areas. On the other hand, the absence of simulated variability in regions where it is observed indicates that its cause is likely the oceans. For example, the coupled biosphere–atmosphere model simulates very little variability in the equatorial regions making the sea surface temperature variations the most probable cause of the observed long-term variability there (Hastenrath 1991).

Decadal variability of precipitation has been documented in the Sahel and the U.S. Midwest, which may corroborate our hypothesis. Observations (Nicholson 2000) and models (Wang and Eltahir 2000c; Zeng et al. 1999) suggest that vegetation dynamics plays an important role in the Sahel. The mechanism of the decadal variability of the precipitation in the Midwest is still a matter of debate (Hu et al. 1998), however. Our results indicate that vegetation feedbacks might play a role.

Besides the effect of the ocean, there are also processes on land that could alter the variability of the climate. We have only considered natural ecosystems in our study. But managed ecosystems are likely to affect the variability of the climate as well. Wang and Eltahir (2000b) showed, for example, how an increase in grazing practices could have initiated the last drought in the Sahel. Furthermore, many other processes affecting the functioning of terrestrial ecosystems—like soil erosion or natural disturbances—are not represented in this model and could modulate the variability of the climate–biosphere system.

Despite these caveats, an important point is made clear from this study: terrestrial ecosystems may play an important role in enhancing the long-term variability of the climate system. In much the same way as the oceans are thought to influence decadal and centennial climate variability, terrestrial ecosystems can provide a ''memory'' to the climate system, causing important variations of climate and ecological conditions on long time scales. This result suggests the climate system is even more complex than previously thought and that the role of the terrestrial biosphere—in both short-term biophysical processes (such as energy, water, and momentum exchange) and long-term ecological processes—is essential.

Acknowledgments. We thank Mike Coe, Navin Ramankutty, Sam Levis, and Lixin Lu for useful comments on earlier drafts of these manuscripts.

REFERENCES

Amthor, J. S., 1984: The role of maintenance respiration in plant growth. *Plant Cell Environ.,* **7,** 561–569.

Barry, R. G., and A. M. Carleton, 2001: *Synoptic and Dynamic Climatology.* Routledge, 620 pp.

Bonan, G. B., 1998: The land surface climatology of the NCAR Land Surface Model coupled to the NCAR Community Climate Model. *J. Climate,* **11,** 1307–1326.

——, 2002: *Ecological Climatology, Concepts and Applications.* Cambridge University Press, 678 pp.

Botta, A., N. Viovy, P. Ciais, P. Friedlingstein, and P. Monfray, 2000: A global prognostic scheme of leaf onset using satellite data. *Global Change Biol.,* **6,** 709–725.

Brovkin, V., M. Claussen, V. Petoukhov, and A. Ganopolski, 1998: On the stability of the atmosphere–vegetation system in the Sahara/Sahel region. *J. Geophys. Res.,* **103** (D24), 31 613–31 624.

Burroughs, W. J., 1992: *Weather Cycles: Real or Imaginary?* Cambridge University Press, 201 pp.

Claussen, M., C. Kubatzki, V. Brovkin, A. Ganopolski, P. Hoelzmann, and H. J. Pachur, 1999: Simulation of an abrupt change in Saharan vegetation in the mid-Holocene. *Geophys. Res. Lett.,* **26,** 2037–2040.

Collatz, G. J., J. T. Ball, C. Grivet, and J. A. Berry, 1991: Physiological and environmental regulation of stomatal conductance, photosynthesis and transpiration—A model that includes a laminar boundary-layer. *Agric. For. Meteor.,* **54,** 107–136.

——, M. Ribas-Carbo, and J. A. Berry, 1992: Coupled photosynthesis-stomatal conductance model for leaves of C_4 plants. *Aust. J. Plant Physiol.,* **19,** 519–538.

Costa, M. H., and J. A. Foley, 1997: Water balance of the Amazon basin: Dependence on vegetation cover and canopy conductance. *J. Geophys. Res.,* **102** (D20), 23 973–23 989.

Delire, C., and J. A. Foley, 1999: Evaluating the performance of a land surface/ecosystem model with biophysical measurements from contrasting environments. *J. Geophys. Res.,* **104** (D14), 16 895–16 909.

——, S. L. Levis, G. Bonan, J. A. Foley, M. T. Coe, and S. Vavrus, 2002: Comparison of the climate simulated by the CCM3 coupled to two different land-surface models. *Climate Dyn.,* **19,** 657–669.

——, J. A. Foley, and S. Thompson, 2003: Evaluating the carbon cycle of a coupled atmosphere–biosphere model. *Global Biogeochem. Cycles,* **17,** 1012, doi:10.1029/2002GB001870.

Delworth, T. L., and S. Manabe, 1988: The influence of potential evaporation on the variabilities of simulated soil wetness and climate. *J. Climate,* **1,** 523–547.

——, and ——, 1989: The influence of soil wetness on near-surface atmospheric variability. *J. Climate,* **2,** 1447–1462.

Farquhar, G. D., S. von Caemmerer, and J. A. Berry, 1980: A biochemical model of photosynthetic CO_2 assimilation in leaves of C_3 species. *Planta,* **149,** 78–90.

Foley, J. A., C. I. Prentice, N. Ramankutty, S. Levis, D. Pollard, S. Sitch, and A. Haxeltine, 1996: An integrated biosphere model of land surface processes, terrestrial carbon balance, and vegetation dynamics. *Global Biogeochem. Cycles,* **10,** 603–628.

——, S. Levis, I. C. Prentice, D. Pollard, and S. L. Thompson, 1998:

Unauthenticated | Downloaded 12/05/21 03:12 AM UTC

Coupling dynamic models of climate and vegetation. *Global Change Biol.,* **4,** 561–579.
——, ——, M. H. Costa, W. Cramer, and D. Pollard, 2000: Incorporating dynamic vegetation cover within global climate models. *Ecol. Appl.,* **10,** 1620–1632.
——, M. T. Coe, M. Scheffer, and G. L. Wang, 2003: Regime shifts in the Sahara and Sahel: Interactions between ecological and climatic systems in northern Africa. *Ecosystems,* **6,** 524–539.
Ghil, M., 2002: Natural climate variability. *Encyclopedia of Global and Environmental Change,* T. Munn, Ed., John Wiley and Sons, 544–549.
——, and Coauthors, 2002: Advanced spectral methods for climatic time series. *Rev. Geophys.,* **40,** 1003, doi:10.1029/2000RG000092.
Global Soil Data Task Group, 2000: Global gridded surfaces of selected soil characteristics. Internationl Geosphere–Biosphere Programme, Data and Information System CD-ROM. [Available online at http://www.daac.ornl.gov.]
Hasselmann, K., 1976: Stochastic climate models. Part I. Theory. *Tellus,* **28,** 473–485.
Hastenrath, S., 1991: *Climate Dynamics of the Tropics.* Kluwer, 488 pp.
Higgins, P. A. T., M. D. Mastrandrea, and S. H. Schneider, 2002: Dynamics of climate and ecosystem coupling: Abrupt changes and multiple equilibria. *Philos. Trans. Roy. Soc. London,* **357,** 647–655.
Hu, Q., C. M. Woodruff, and S. E. Mudrick, 1998: Interdecadal variations of annual precipitation in the central United States. *Bull. Amer. Meteor. Soc.,* **79,** 221–229.
Kiehl, J. T., J. J. Hack, G. B. Bonan, B. A. Boville, D. L. Williamson, and P. J. Rasch, 1998: The National Center for Atmospheric Research Community Climate Model: CCM3. *J. Climate,* **11,** 1131–1149.
Kucharik, C. J., and K. R. Brye, 2003: Integrated Biosphere Simulator (IBIS) yield and nitrate loss predictions for Wisconsin maize receiving varied amounts of nitrogen fertilizer. *J. Environ. Quality,* **32,** 247–268.
——, and Coauthors, 2000: Testing the performance of a dynamic global ecosystem model: Water balance, carbon balance, and vegetation structure. *Global Biogeochem. Cycles,* **14,** 795–825.
——, K. R. Brye, J. M. Norman, J. A. Foley, S. T. Gower, and L. G. Bundy, 2001: Measurements and modeling of carbon and nitrogen cycling in agroecosystems of southern Wisconsin: Potential for SOC sequestration during the next 50 years. *Ecosystems,* **4,** 237–258.
Lenters, J. D., M. T. Coe, and J. A. Foley, 2000: Surface water balance of the continental United States, 1963–1995: Regional evaluation of a terrestrial biosphere model and the NCEP/NCAR reanalysis. *J. Geophys. Res.,* **105** (D17), 22 393–22 425.
Levis, S., J. A. Foley, V. Brovkin, and D. Pollard, 1999a: On the stability of the high-latitude climate–vegetation system in a coupled atmosphere–biosphere model. *Global Ecol. Biogeogr.,* **8,** 489–500.
——, ——, and D. Pollard, 1999b: CO_2, climate, and vegetation feedbacks at the Last Glacial Maximum. *J. Geophys. Res.,* **104** (D24), 31 191–31 198.
——, ——, and ——, 1999c: Potential high-latitude vegetation feedbacks on CO_2-induced climate change. *Geophys. Res. Lett.,* **26,** 747–750.
——, ——, and ——, 2000: Large-scale vegetation feedbacks on a doubled CO_2 climate. *J. Climate,* **13,** 1313–1325.
Liu, Y. Q., and R. Avissar, 1999: A study of persistence in the land–atmosphere system using a general circulation model and observations. *J. Climate,* **12,** 2139–2153.
Manabe, S., and R. J. Stouffer, 1996: Low-frequency variability of surface air temperature in a 1000-year integration of a coupled atmosphere–ocean–land surface model. *J. Climate,* **9,** 376–393.
Mitchell, J. M., 1976: An overview of climatic variability and its casual mechanisms. *Quat. Res.,* **6,** 481–493.
Namias, J., 1952: The annual course of month-to-month persistence in climatic anomalies. *Bull. Amer. Meteor. Soc.,* **33,** 279–285.
Nemani, R. R., C. D. Keeling, H. Hashimoto, W. M. Jolly, S. C. Piper, C. J. Tucker, R. B. Myneni, and S. W. Running, 2003: Climate-driven increases in global terrestrial net primary production from 1982 to 1999. *Science,* **300,** 1560–1563.
Nicholson, S., 2000: Land surface processes and Sahel climate. *Rev. Geophys.,* **38,** 117–139.
Ramankutty, N., and J. A. Foley, 1999: Estimating historical changes in global land cover: Croplands from 1700 to 1992. *Global Biogeochem. Cycles,* **13,** 997–1027.
Scheffer, M., S. Carpenter, J. A. Foley, C. Folke, and B. Walker, 2001: Catastrophic shifts in ecosystems. *Nature,* **413,** 591–596.
Thompson, S. L., and D. Pollard, 1995a: A global climate model (GENESIS) with a land-surface transfer scheme (LSX). Part I: Present climate simulation. *J. Climate,* **8,** 732–761.
——, and ——, 1995b: A global climate model (GENESIS) with a land-surface transfer scheme (LSX). Part II: CO_2 sensitivity. *J. Climate,* **8,** 1104–1121.
Wang, G., and E. A. B. Eltahir, 2000a: Biosphere–atmosphere interactions over West Africa. II: Multiple climate equilibria. *Quart. J. Roy. Meteor. Soc.,* **126,** 1261–1280.
——, and ——, 2000b: Ecosystem dynamics and the Sahel drought. *Geophys. Res. Lett.,* **27,** 795–798.
——, and ——, 2000c: Role of vegetation dynamics in enhancing the low-frequency variability of the Sahel rainfall. *Water Resour. Res.,* **36,** 1013–1021.
——, ——, J. A. Foley, D. Pollard, and S. Levis, 2004: Decadal variability of rainfall in the Sahel: Results from the coupled GENESIS–IBIS atmosphere–biosphere model. *Climate Dyn.,* **22,** doi:10.1007/s00382-004-0411-3.
Zeng, N., J. D. Neelin, K. M. Lau, and C. J. Tucker, 1999: Enhancement of interdecadal climate variability in the Sahel by vegetation interaction. *Science,* **286,** 1537–1540.

Unauthenticated | Downloaded 12/05/21 03:12 AM UTC